Transportation Infrastructure Precast Innovation Center (TRANS-IPIC)

University Transportation Center (UTC)

Adaptive camber precast concrete girder for deflection mitigation of highway bridges

Project # UI-23-RP-04

Quarterly Progress Report

For the performance period ending September 30, 2024

Submitted by:

Ann C. Sychterz, Assistant Professor, Civil and Environmental Engineering,

University of Illinois Urbana-Champaign, asychter@illinois.edu

Collaborators / Partners:

Jacob Henschen, Teaching Assistant Professor, Civil and Environmental Engineering,
University of Illinois Urbana-Champaign, jhensche@illinois.edu

Submitted to:

TRANS-IPIC UTC

University of Illinois Urbana-Champaign

Urbana, IL

TRANS-IPIC Quarterly Progress Report:

Project Description:

1. Research Plan - Statement of Problem
   The vision of this work is that through innovative use of mechanical anchors, precast concrete bridge girders can adaptively camber to have zero deflection when subjected to external loads. Motivation for this work is twofold: topology optimization and long-term deflection control for transforming precast concrete research. A bridge girder that contains the science of adding camber when loads are applied can reduce girder depth for stiffness requirements, optimizing material utilized as a sustainable solution in the light of climate change. Anchors inserted into slots along the top face of the girder expand longitudinally in the compression zone of the girder when vertical load is applied. The objectives of this proposed work are: 1) create a time-domain quasi static model for load-dependent adaptive camber concrete beam, and 2) compare and validate the model with experimental measurements of adaptive camber beam subjected to gravity and moving loads.

2. Research Plan - Summary of Project Activities (Tasks)

   Task 1.1: Model stress distribution in precast concrete adaptive girder due to exerted force from adaptive anchor system. A finite element model will be created to characterize the stress distribution in the girder as a camber is forced into the compression face. Anchors will be embedded into slots on the top face of the precast girder.

   Task 1.2: Create form-finding model of time-varying camber of adaptive precast girder. A form finding method, called dynamic relaxation, is a static analysis that does not require inversion of the stiffness matrix, thus well-suited for structures undergoing large deformations. This method is better suited to large deformations compared with finite element models for the structural member.

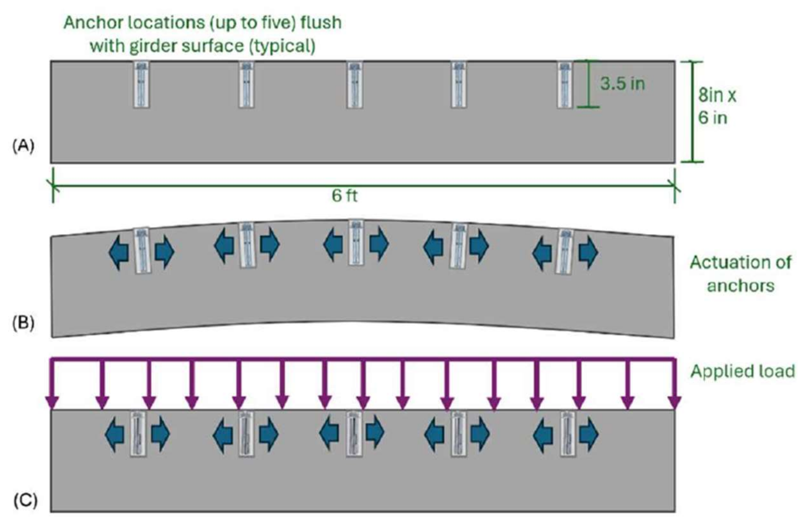

Figure 1: System concept for adaptive precast concrete girder. Embedded anchors are inactive when there is no load (a) and actively cause camber when load is applied (b) and final form (c).

Task 2.1: Study adaptive camber effect of one anchor for parametric analysis. To examine the experimental behavior of the expanding anchor that will form the basis of the adaptive precast girder system, stress and strain from one expanding anchor will be studied. A specimen of approximately 1-ft span and 4-in depth will be formed with one slot on the compression face for an anchor of approximately 1-in length.

Task 2.2: Build 2-ft prototype of adaptive precast concrete girder and compare measurements with analytical model. A bench-scale precast girder will be approximately 4-ft span and a cross-section of 6-in depth and 4-in width. Minimum longitudinal tensile reinforcement will be provided. Strain gauges and high-fidelity camera measurements will be utilized for data collection during testing in the same manner as in Task 2.1.

Project Progress:

3. Progress for each research task

   Task 1.1: 100% complete: Figure 1 shows the adaptive concrete beam concept with expanding elements (anchors or lab jack) in the compression face of the beam. A preliminary 2D finite element model was built in Abaqus of the proposed reinforced concrete specimen of 16 in span by a square cross section of 4 in. The concrete had a concrete strength of 3 ksi and a density of 150 pcf. The model was simply supported on each end of the span and the actuation was located at the top face at midspan. The maximum force capable of the lab jack from Task 2.2 was utilized in this model to calculate the maximum possible camber in the finite element model.

   RESULTS: Figure 2 shows the finite element model of the concrete beam specimen and was modeled as a thick shell element in SAP2000. Under self-weight, the deflection was 0.000056 in at the bottom of the plate. Applying the 91 lbs of force at the top face of the structure, the upwards camber was a maximum of 0.00016 in. Since actuation causes larger displacements, finite element models cannot be utilized throughout the process, therefore, a form-finding model is effective to impose incremental elongation of the lab jack and deployable anchor.

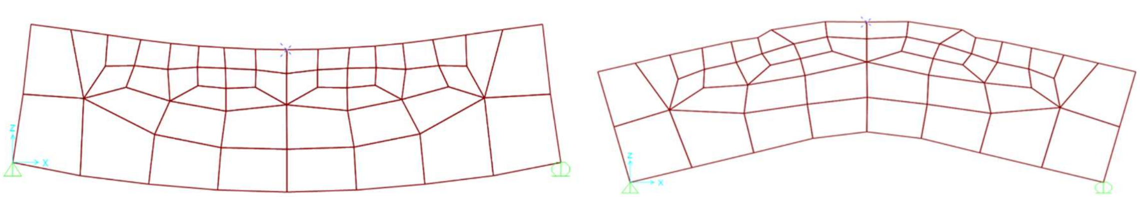

a) Self-weight deflection of 0.000056 in of the beam.

b) Actuation camber of 0.00016 in from lab jack force of 22 lb.

Figure 2: Results from finite element thick shell analysis of the adaptive concrete specimen.

   Task 1.2: 90% complete: A form finding method, called dynamic relaxation, is a static analysis that does not require inversion of the stiffness matrix, thus well-suited for structures undergoing large deformations. This method is better suited to large deformations compared with finite element models for the structural member. The model leverages a strut-and-tie model of the concrete specimen with an additional element for actuation at the center where the expanding system is installed. The specimen boundary conditions are restrained for out-of-plane movement and simply supported at the ends of the beam as shown in Figure 3. The dynamic relaxation model utilized the same material properties as given for the finite element model. The #2 reinforcement placed at the bottom of the specimens is 60 ksi reinforcement steel. Activation of the anchors in the compression zone will be simulated in a stepwise manner, ignoring inertial effects of shock loading. The actuation element is infinitely stiff and is studied in increments of 0.5 in up to a maximum of 8 in, governed by the maximum expansion of the lab jack.

RESULTS: Due to the research gap of form-finding methods not being implemented for origami, this provides an opportunity to modify the dynamic relaxation algorithm for the case of the actuated concrete structure. This section discusses the modification of the dynamic relaxation algorithm where the angle stiffness, K_B for bending, is an input to the simulation. Implementation of friction at nodes occurs in the calculation of residual forces due to angle stiffness and affects the balance of internal forces in the concrete beam. Dynamic relaxation is a static analysis however it includes fictitious inertia and damping terms. With these terms, an augmented equation of motion is used to determine a new static equilibrium of the artificially damped structure.

The fictitious mass matrix calculation improves kinetic damping and thus convergence of the algorithm. Underwood *(28)* proposed a theorem using the upper bounds of the recurrence matrix $\mathbf{M}^{-1}\mathbf{K}$, where **M** is the mass matrix and **K** is the stiffness matrix. For the stability of a given time step, δt, **Equation 1** must be satisfied to guarantee stability where $k_{i,j}$ are elements of the tangent stiffness matrix.

$$M_i = \frac{1}{4}\delta t^2 \sum_j |k_{i,j}| \tag{1}$$

The contributions from all members meeting at the node for a given direction, x, are calculated using **Equation 2**.

$$M_{i,x} = \left(\frac{\delta t}{2}\right)^2 \frac{k_{i,j}}{2} \tag{2}$$

The modification introduced to dynamic relaxation is concerned with the calculation of the angle stiffness within the calculation of residual forces. Each node is surveyed, first retrieving the displacements for the current node i. Angle stiffness value K_B, element ID and nodal coordinates that are connected to current node i, and elements that define the type of angles at node i are retrieved as these values are calculated outside the residual force convergence loop of the dynamic relaxation algorithm. For every angle, one element defines the vertex bend line, $\vec{v}$, and two elements define rays, $\vec{u}$ and $\vec{w}$ for the angle in Euclidean space.

The angle is determined by the normal to planes, $\vec{n}$ and $\vec{m}$ formed by the vertex bend line and a ray, and then calculating the inverse tangent of the normalized cross product of the planes divided by the dot product of the planes. This procedure is carried out for all nodes for bending. A check is then made to determine if the angle is the same at both ends of the element, θ_i and θ_{i+1}. These two angle values are used to determine if the structure is deforming. The angle values are stored as initial values and compared with the previous steps to calculate the incremental angle change, $\Delta\theta_i$, to calculate the change in force in **Equation 3**.

(3)

$$F_{KB,i} = K_B * \Delta\theta_{B,i}$$

Variable $F_{KB,i}$ is the force resisting rotation due to bending stiffness at a node i. Change in angle at node i between two actuation steps is denoted $\Delta\theta_i$. This angle force is distributed to the elements that connect to current node i, proportional to their length in **Equation 4.**

$$F_{KB,i,m} = F_{KB,i} * \frac{l_m}{\sum_1^M l_m} \tag{4}$$

Index l_m indicates length of a member connected to node i, with a total of M connected members. These values are then combined with the residual force calculation of the dynamic relaxation algorithm (**Equation 5**).

$$f_{ext,i,x} = f_{ext,i,x} + F_{KB,i,m} \tag{5}$$

Residual forces $R_{i,x}^t$ of member m at time step t is the sum of external forces and the x-component of resultant forces by N_m members meeting at node i. The ratio of element tension u_m^t, and length of member l_m^t is multiplied by the x-coordinates of nodes i and j of the member (**Equation 6**). This process is repeated for all coordinate directions.

$$R_{i,x}^t = f_{ext,i,x} + \sum_{m=1}^{N_m} \frac{u_m^t}{l_m^t}\left(x_{j,m}^t - x_{i,m}^t\right) \tag{6}$$

A model is created to characterize the stress distribution in the girder as a camber is forced into the compression face. Anchors are be embedded into slots on the top face of the precast girder. This model targets stress distributions around the slots that inform the design of anchor spacing. The finite element model is used to calculate the maximum analytical camber force that can be exerted on the precast girder due to local effects around the anchor.

A form finding method, called dynamic relaxation, is a static analysis that does not require inversion of the stiffness matrix, thus well-suited for structures undergoing large deformations. This method is better suited to large deformations compared with finite element models for the structural member (**Figure 3).** The strut-and-tie method was used for approximating the cross-sectional area of the struts of 9 in^2. Activation of the anchors in the compression zone are simulated in a stepwise manner, ignoring inertial effects of instantaneous loading. This analysis provides the system-level camber behavior from the expanding anchors adding compression to the compression zone of the

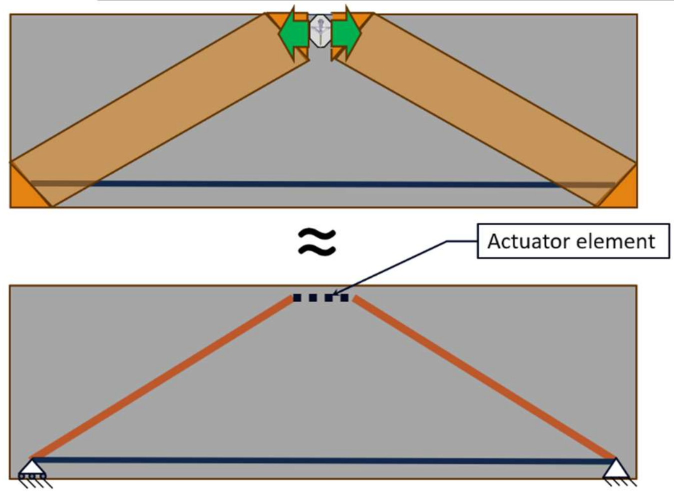

Figure 3: Comparison of a strut-and-tie concrete model with compression struts (orange) and tension ties (blue) due to applied load [top]. The dynamic relaxation formulation has axial elements in the same color scheme with an additional actuator element (black dashed) to simulate the expanding anchor or jack.

experimental girder. Rotational springs at the hinges were required for his structure to prevent a 4-bar linkage kinematic instability, therefore the formulation of dynamic relaxation with spring hinges for origami by the authors was implemented.

Forces in the compression members per inch of actuation of anchor or lab jack results in approximately 295 lb axial force which is 1.1% of the utilization ratio, demand per capacity, of the structure. Therefore, testing of the adaptive concrete structure is non-destructive and repeatable, which is useful for future large-scale tests. The rotational hinge stiffness, K_B, for the nodes at the support was a function of the mean moment of inertia multiplied by the Young's Modulus of Elasticity of the elements joining at a given node, which is approximately 10.5 kN-in^2. For the nodes adjacent to the actuator, the bending stiffness is only related to the concrete struts as the actuator has a representative stiffness and area, which is approximately 21 kN-in^2.

Task 2.1: 100% complete

The stress distribution within the section was analyzed using fundamental principles of reinforced concrete design. Through the dimensions shown in Figure 4, the maximum compressive force that could be exerted from the lab jack is 22 lbs given the surface area and location above the neutral axis of the concrete specimen.

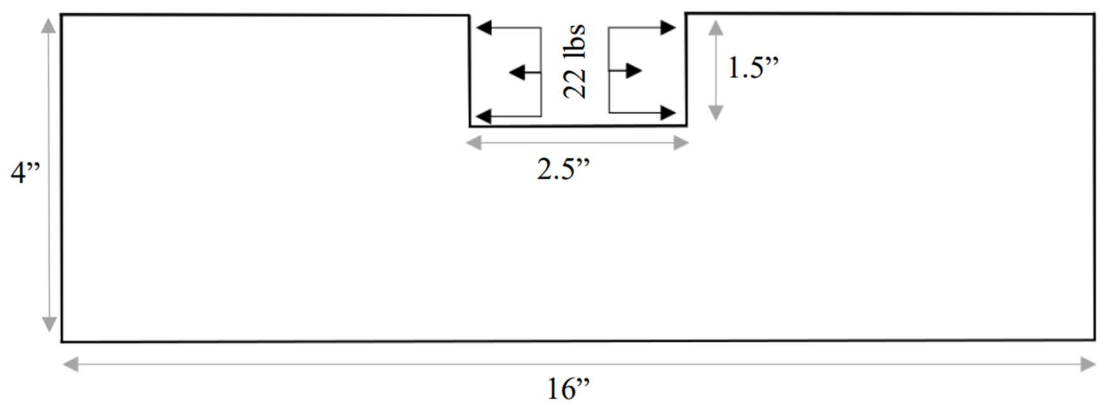

Figure 4: Elevation view of the concrete specimen with the maximum compressive force available from the lab jack to be applied in the compression zone for adaptive camber.

RESULTS: Figure 5 shows the strain field of the beam with the lab jack (a) and 0.25 in anchors (b) during applied loading. The maximum force from the lab jack that was measured in the experimental tests, discussed below, was 91 lb. This force was applied on the inside vertical faces of the notch in the beam in the model and compared to the experimental strains. It was found that the model and measurements were in agreement with an error of less than 5%, which was deemed acceptable. Since the applied load of the anchors was not directly measurable, the inverse problem was solved using the maximum strain due to the anchors. It was determined that the exerted force from the 0.25 in anchors is 200 lbs. Although this is a thick shell model, strain values are within the same magnitude for their respective regions on the experimental prototype, shown in the following sections.

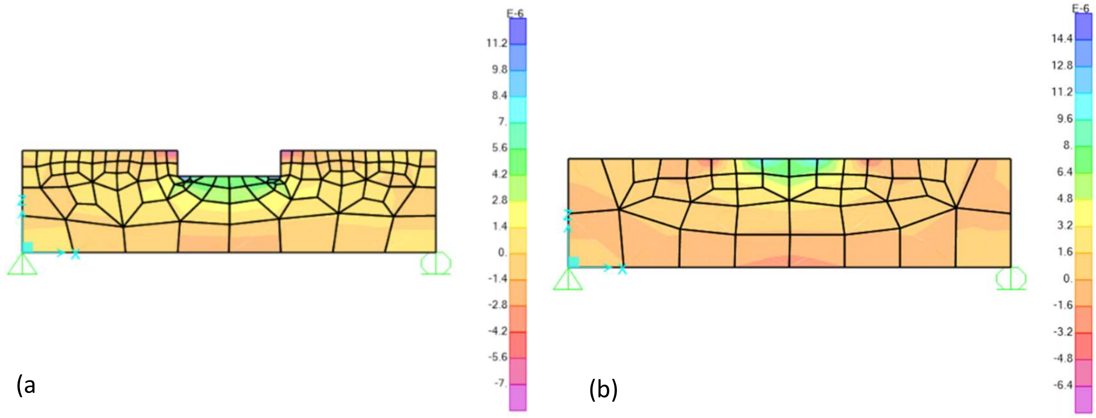

Figure 5: Strain field for maximum lateral force of (a) lab jack and (b) 0.25 in anchors.

Task 2.2: 100% complete

Prior to installation of the anchors in the specimens, the expanding wall anchors had to be tested for their capability to provide lateral forces when they are activated. These wall anchors are specified for their pull-out strength perpendicular to the surface they are anchored, but not the lateral pressure. Therefore, a masters semester project in Fall 2023 was conducted to study the split-sleeve and winged anchor lateral force capacity.

Concrete specimens of a 16 in span, and a 3 in by 4 in section were cast in the concrete lab at the University of Illinois under the supervision of Prof. Henschen. The specimens were cast of normal weight concrete, targeting a 4 ksi strength (Table 1). Polypropolene fiber reinforcement (<0.05% by volume) was used to prevent brittle failure in laboratory testing but would not affect the compressive or tensile behavior. Two #2 steel reinforcement bars were placed at the bottom of the specimen for tensile resistance of the section.

Table 1: Concrete constituents

	Units	Quantity
Cement	lb/ft^3	21.4
Coarse Aggregate	lb/ft^3	69.8
Fine Aggregate	lb/ft^3	46.7
Water	lb/ft^3	12.7
Superplasticizer	fl oz/cwt	3.0
Fibers	lb/ft^3	2.0
Slump	in	5.5
Air content	%	1.5

RESULTS: Out of the tested anchors (hollow-wall and sleeve anchors), the hollow-wall anchors are the only anchor which produced measurable forces on the food scale. The sleeve anchors did not produce results using this test method and must be tested in another manner. The hollow-wall anchors produced 12 force readings. A scatter plot of Force vs Test Number is shown in Figure 6.

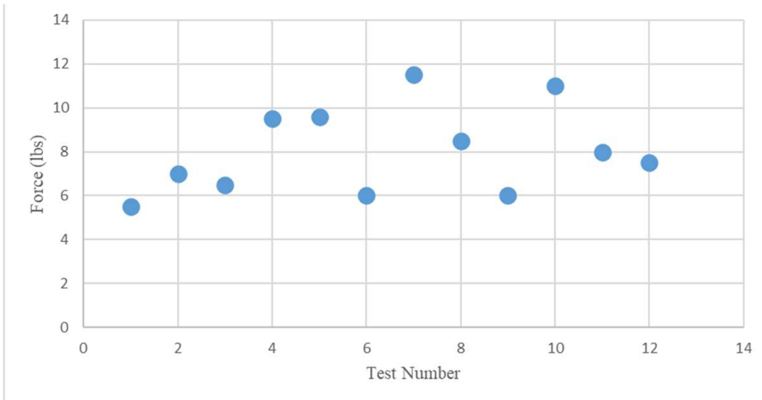

Figure 6: Lateral Force Capacity for the Hollow-Wall Anchors

Through twelve tests, force values ranged from 5.5-11.5 pounds producing a range of 6 pounds. The average of tests was 8.05 pounds with a standard deviation of 2 pounds. Testing the anchors using the wood produced results for the hollow wall anchor, but not for the sleeve anchor. The sleeve anchor was expanded fully and remained flush within the test frame but did not produce force on the scale. Sleeve anchors do not deploy in large deformations or high rates, which may have allowed the top plate to slip upward under the gradual application of force.

Concrete specimens were cast as shown in Figure 7 [left] and instrumented with strain gauges [right].

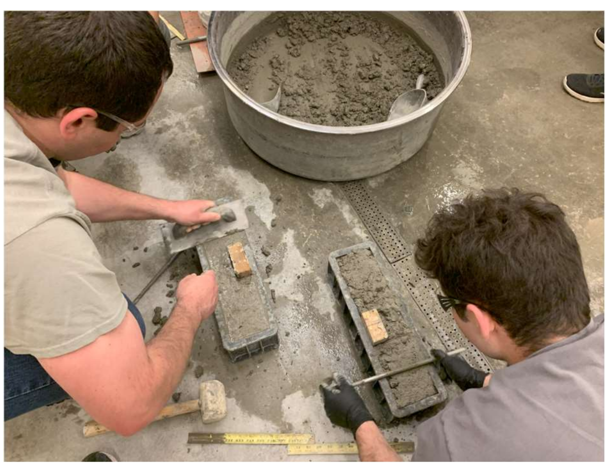

Figure 7: Casting of concrete specimens [left] and instrumentation [right].

Figure 8 shows the concrete specimens when the installation of the lab jack in the compression zone expanding longitudinally along the beam. Strain gauge data results from these actuation tests are shown in Figure 9.

Figure 8: Experimental setup with the lab jack as the actuator.

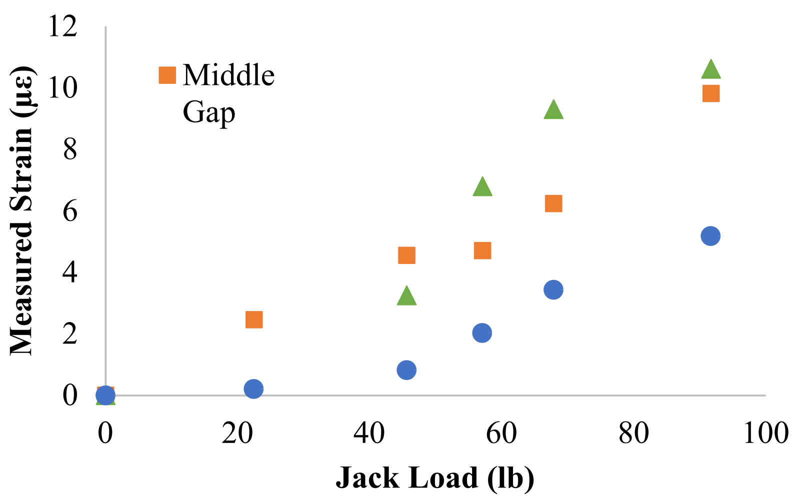

Figure 9: Measured strain as a function of the applied load from the lab jack.

The experimental setup of the actuation with deployable anchors in the concrete specimens are shown in Figure 10. Strain gauge results from the actuation of the deployable anchors is shown in Figure 11, Figure 12 and Figure 13 .

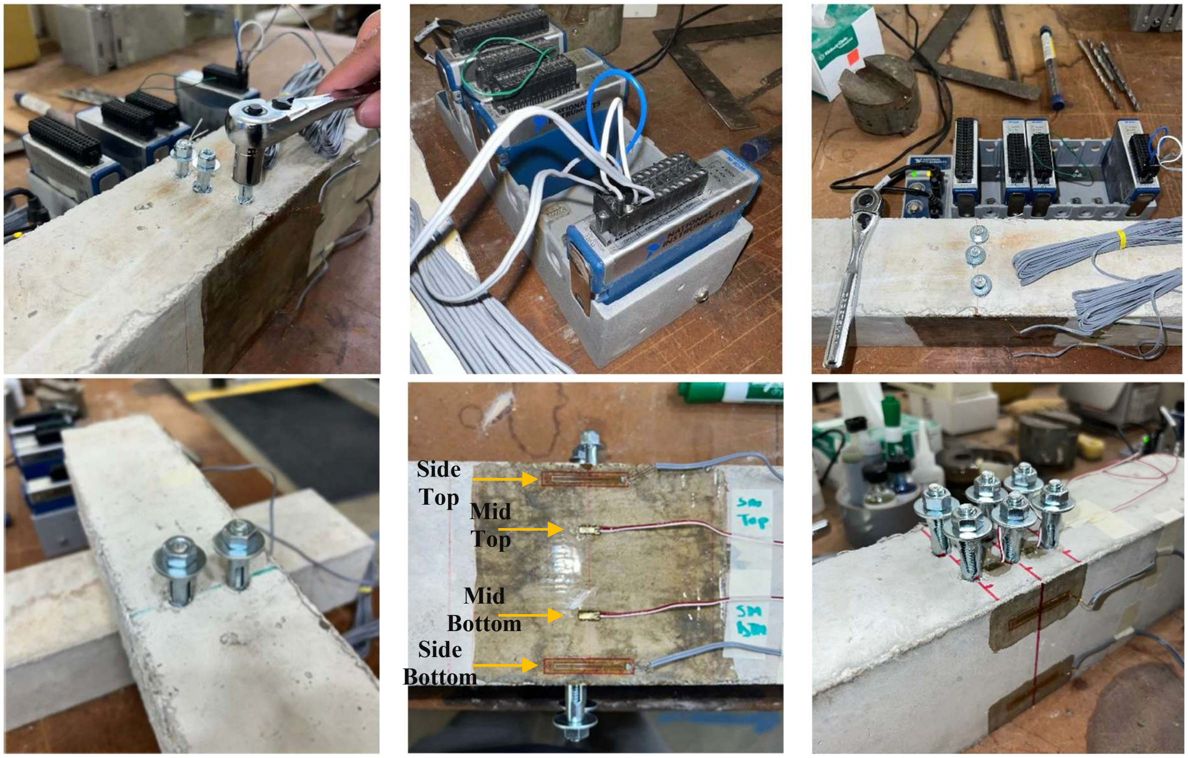

Figure 10: Deployable a row of 3-0.25 in. anchors being installed into the concrete specimen 1 [top-left]. Data acquisition system for the test setup collects strain of the concrete [top-center] and top view of the anchor installation with at least 1 in separation between the anchors at the midspan region of interest [top-right]. Deployable a row of 2-0.375 in. anchors being installed into the concrete specimen 2 [bottom-left]. Beam side face with the 4 strain gauges locations [bottom-center] Deployable a row of 3-0.375 in. anchors being installed into the concrete specimen 3 [bottom-right].

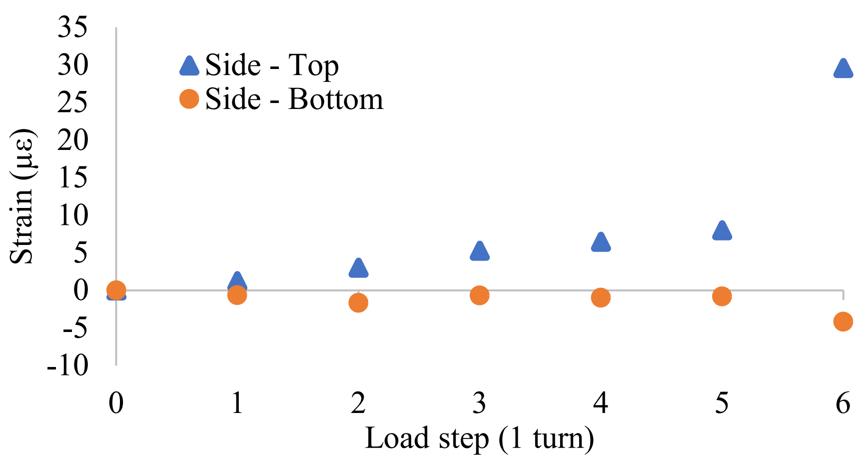

Figure 11: Measured strain as a function of tightening the 0.25 in. anchor.

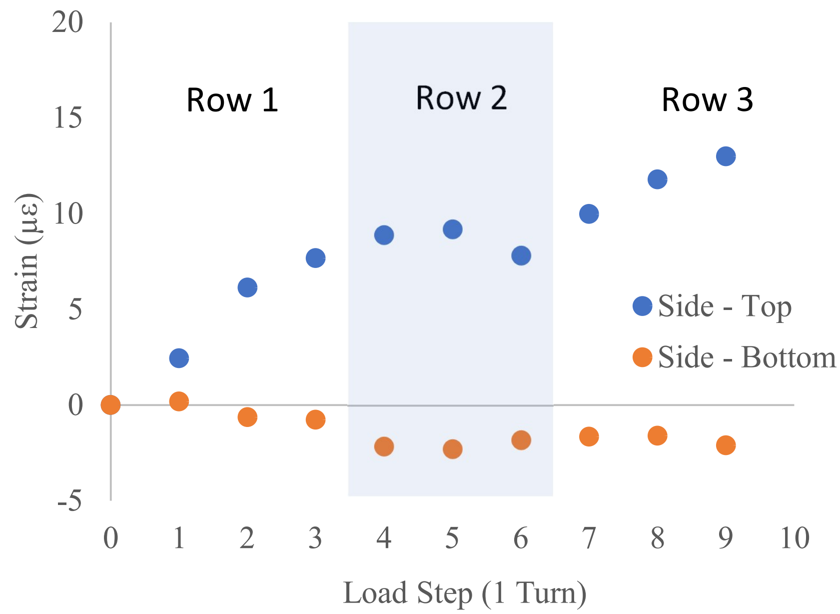

Figure 12: Measured strain as a function of tightening of 3 rows of 0.375 in. anchors

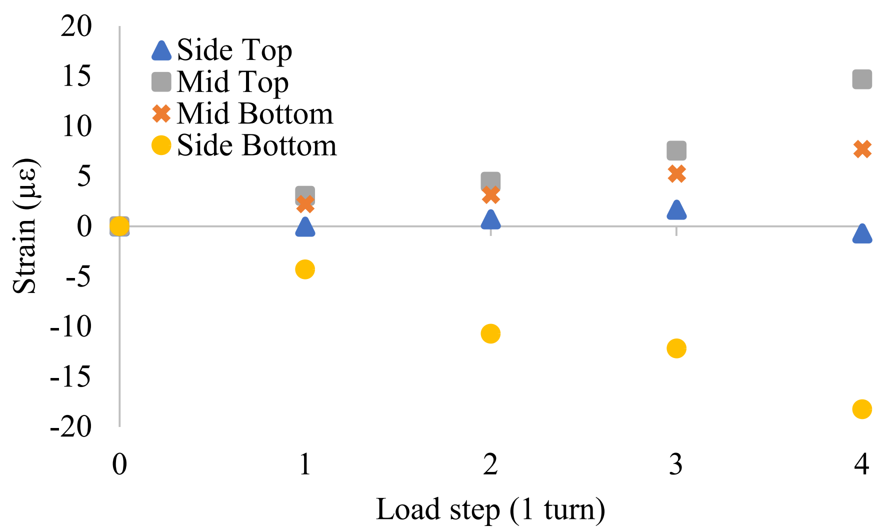

Figure 13: Measured strain as a function of tightening the 0.375 in. anchor.

The experimental setup of the actuation with 9 deployable anchors in the new concrete specimen is shown in Figure 14. For this specimen, an LVDT sensor was used to accurately measure deflection at each step as the anchors were tightened incrementally. The strain gauge results from the actuation of the deployable anchors, along with the corresponding deflection measurements recorded by the LVDT sensor, are displayed in table 2.

Figure 14: Deployable a 3 rows of 9-0.375 in. anchors being installed into the concrete specimen 4 [left]. LVDT displacement/voltage data collecting [center] and front view of the anchor installation with and LVDT sensor on specimen 4 [right].

Table 2: Strain gauge data from actuation of concrete specimen 4 with anchors / LVDT data

Strain gauge test output for Beam 4 (9 (9-Mid / 9-Right / 9-left) Expantion Anchors - Hex Head 3/8") / LVDT					
Anchors Tighten Strength	Strain No.	Strain Location	CH. No.	StrainTest Results	LVDT Voltage
No Load	1	Side face - Top	0	1.3868 m	-1.088
	2	Side face - Bottom	1	40.3535 u	
1	1	Side face - Top	0	1.3857 m	-1.0887
	2	Side face - Bottom	1	38.9321 u	
2	1	Side face - Top	0	2.8109 m	-1.0887
	2	Side face - Bottom	1	35.7374 u	
3	1	Side face - Top	0	2.8163 m	-1.0893
	2	Side face - Bottom	1	36.4456 u	
4	1	Side face - Top	0	2.8217 m	-1.0883
	2	Side face - Bottom	1	33.7812 u	
5	1	Side face - Top	0	2.8217 m	-1.0882
	2	Side face - Bottom	1	32.5216 u	
6	1	Side face - Top	0	2.8283 m	-1.089
	2	Side face - Bottom	1	31.4872 u	
7	1	Side face - Top	0	2.8380 m	-1.0883
	2	Side face - Bottom	1	29.0279 u	
8	1	Side face - Top	0	2.8576 m	-1.0913
	2	Side face - Bottom	1	36.0435 u	
9	1	Side face - Top	0	2.8654 m	-1.0965
	2	Side face - Bottom	1	42.2992 u	
10	1	Side face - Top	0	2.8736 m	-1.0883
	2	Side face - Bottom	1	45.9127 u	
11	1	Side face - Top	0	2.8752 m	-1.0885
	2	Side face - Bottom	1	45.9092 u	
12	1	Side face - Top	0	2.8987 m	-1.0882
	2	Side face - Bottom	1	46.2047 u	
13	1	Side face - Top	0	2.9064 m	-1.8817
	2	Side face - Bottom	1	46.5742 u	
14	1	Side face - Top	0	2.9063 m	-1.0892
	2	Side face - Bottom	1	38.9884 u	
15	1	Side face - Top	0	2.9077 m	-1.0894
	2	Side face - Bottom	1	37.8594 u	

LVDT	
Dispalcement (in.)	Voltage
-8.13	-1.0872
-8.15	-1.086
-8.175	-1.084
-8.2	-1.0812
-8.225	-1.0788
-8.25	-1.0763
-8.275	-1.0741
-8.3	-1.0711
-8.325	-1.0685
-8.35	-1.0663
-8.375	-1.0637
-8.4	-1.0611
-8.425	-1.0581
-8.45	-1.0557
-8.475	-1.0537
-8.5	-1.0504
-8.525	-1.0479
-8.55	-1.0456
-8.575	-1.0435
-8.6	-1.0407
-8.625	-1.0382
-8.65	-1.0366
-8.675	-1.0343
-8.7	-1.0323
-8.725	-1.0297
-8.75	-1.0286
-8.775	-1.0266
-8.8	-1.0249
-8.825	-1.0238
-8.85	-1.0221
-8.875	-1.021
-8.885	-1.2067

Response to Reviewer from Q3 report: These strain gauge and displacement results show that a reasonable number of anchors for the length of the specimen are successfully cambering the beam. This addresses the objective of the project to be able to reduce the cross section of the concrete member with an adjustable prestress to counteract self-weight (superimposed dead loads and moving loads will be completed in the next quarter).

4. Percent of research project completed
   95%

5. Expected progress for next quarter
   Next quarter will to be complete the dynamic relaxation code to analyze the concrete member as a strut-and-tie model with springs at the nodes for resistance. While the framework is present and working for this code, improvements to the formulation of the spring stiffness would allow the team to compare the results of the dynamic relaxation model to the experimental results. PI Sychterz is working with a MS graduate student for this refinement of the dynamic relaxation model. Static and moving loads will be applied to the model and the experimental prototype to measure the resulting deflection.

6. Educational outreach and workforce development

A) Educational seminar on adaptive concrete research in CEE 465 – Design of Structural Systems, Urbana, IL

PI Sychterz utilized an hour of her lecture time of the senior year integrated design course to discuss the work of TRANS-IPIC and her project on adaptive concrete highway bridge girders as it pertains to structural systems. This occurred in the Fall 2024 semester in the second week of class to introduce the concept of precast concrete structural systems.

B) Student Work and Educational Outreach Presented at ASCE Engineering Mechanics Institute Conference 2024, Chicago, IL

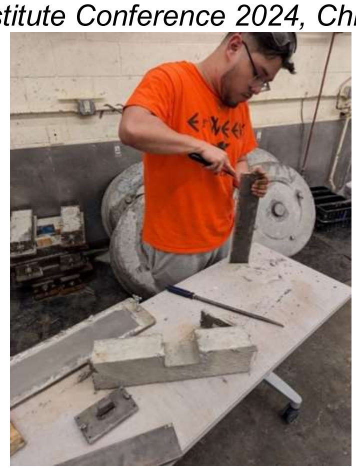

Figure 15: [left] Undergraduate semester project casting concrete specimens and [right] PI Sychterz presenting the preliminary findings at the ASCE Engineering Mechanics Institute Conference in Chicago, May 29, 2024.

Through this research initiative, three undergraduate student semester projects were supported in Spring 2024 (Figure 15) and one masters student semester project in Summer 2024. The undergraduate students worked in a team to cast the concrete specimens for testing as well as calculating, using fundamentals of reinforced concrete design, to calculate the theoretical forces needed for camber in the concrete section to achieve up to 0.5 in of camber. The masters semester project was laboratory-based for installing strain gauges and measuring the deformation of the concrete specimen with actuation.

C) Actuation in Structural Engineering training, University of Illinois Urbana-Champaign, Urbana, IL. In December 2024, PI Sychterz is planning to host a session on Actuation in Structural Engineering training, leveraging the work from this TRANS-IPIC project. The goal of this work is the train students to think about kinematics in elements such as precast concrete. The debrief of this event will be shared with structural engineering collaborator **Jim Pawlikowski, SE, PE LEED AP** who is a Principal at Datum Engineers in Chicago and an expert in concrete construction. PI Sychterz will work towards workforce training in the last quarter of the project about tunable camber in precast concrete.

7. Technology Transfer

   PI Sychterz met with the research and development team of Hilti Group in Schaan, Liechtenstein to propose a joint initiative on anchor testing and development for the future year of work. Although no new design for an anchor has been developed, it is projected that this work could be the catalyst for a **new anchor design patent within the next 5 years.**

   PI Sychterz met with Apolinar Martinez from Utility Concrete Products, a precast concrete company in Illinois to discuss a partnership for the future year of research where industry would serve as an advisory board to PI Sychterz and co-PI Henschen's work with graduate and undergraduate students in the lab. This position on an advisory board would be in hopes of a smooth transfer of the research by Sychterz and Henschen into practice that addresses the fundamental challenges of precast design for highway bridges.

Research Contribution:

8. Papers that include TRANS-IPIC UTC in the acknowledgments section:
   Alotaibi, A., Naranjo, M., Henschen, J., and Sychterz A.C. ADAPTIVE CAMBER OF A CONCRETE GIRDER FOR DEFLECTION MITIGATION, Transportation Research Board Annual Meeting 2025, Washington DC (In review).

   Alotaibi, A., Sychterz A.C, and Henschen, J. Computational Modeling of an adaptive concrete highway bridge girder, American Concrete Institute Conference Spring 2025, Toronto, Canada (In preparation).

9. Presentations and Posters of TRANS-IPIC funded research:
   Sychterz, A.C. Engineering Mechanics Institute 2024, May 29 2024, Chicago, IL, MS0102 Geometries and Design.

   Sychterz, A.C. Adaptive Lightweight Infrastructure (part of seminar talk), June 15 2024, Stuttgart, Germany, University of Stuttgart.

   Sychterz, A.C. Adaptive Lightweight Infrastructure (part of seminar talk), November 7 2024, University of Wisconsin Madison.

   Sychterz, A.C. Adaptive Lightweight Infrastructure (part of seminar talk), June 22, 2025, Laval University, Quebec City, Canada.

   Sychterz, A.C. Adaptive Camber of a Concrete Girder for Deflection Mitigation, Transportation Research Board Annual Meeting 2025 (anticipated).

10. Please list any other events or activities that highlights the work of TRANS-IPIC occurring at your university (please include any pictures or figures you may have). Similarly, please list any references to TRANS-IPIC in the news or interviews from your research.

    TRANS-IPIC was present for the Grainger Engineering ‘City Designers and Builders’ Summer Camp session entitled “Building With Memory” with Prof. Andrawes. It is planned that this research team of Prof. Sychterz and Prof. Henschen will contribute to next summer’s Grainger Engineering Summer Camp while representing TRANS-IPIC. This camp module will address shape-changing structures such as origami structures, tensegrity structures, and how these advanced kinematic structures can be applied to civil engineering systems such as bridge girders.
    https://trans-ipic.illinois.edu/news/2024-CEE-Summer-Camp

    Additionally, there will be a TRANS-IPIC hosted Transportation Infrastructure Precast Day (TIP day) at the University of Illinois Urbana-Champaign campus to bring industry experts to the civil engineering student community to discuss the latest technologies in precast concrete (planned November 1, 2024).

<u>**References:**</u>

Akgün, Y., Gantes, C. J., Sobek, W., Korkmaz, K., & Kalochairetis, K. (2011). A novel adaptive spatial scissor-hinge structural mechanism for convertible roofs. *Engineering Structures*, *33*(4), 1365–1376. https://doi.org/10.1016/j.engstruct.2011.01.014

Pellegrino, S. (2001). *Deployable Structures*. Springer-Verlag.

Reksowardojo, A. P., Senatore, G., & Smith, I. F. C. (2020). Design of Structures That Adapt to Loads through Large Shape Changes. *Journal of Structural Engineering*, *146*(5). https://doi.org/10.1061/(asce)st.1943-541x.0002604

Yin, L., & Ananthasuresh, G. K. (2003). Design of distributed compliant mechanisms. *Mechanics Based Design of Structures and Machines*, *31*(2), 151–179. https://doi.org/10.1081/SME-120020289.

Precast, Prestressed Bridge Girders." (August).

Brown, K. M. (1998). "Camber growth prediction in precast prestressed concrete bridge girders." (December).

French, C. E., and O'Neill, C. R. (2012). "Validation of Prestressed Concrete I-Beam De ection and Camber Estimates." (June), 205.

Honarvar, E., Nervig, J., and Rouse, J. M. (2015). *Improving the accuracy of camber predictions for precast pretensioned concrete beams. DOT National Transportation Integrated Search - ROSA P*.

Precast/Prestressed Concrete Institute. (2018). *Guidelines for Camber and Profile Management in Adjacent Beams*.

Stallings, J. M., Barnes, R. W., and Eskildsen, S. (2003). "Camber and Prestress Losses in Alabama HPC Bridge Girders." *PCI Journal*, 48(5), 90–104.

(2017). *PCI Design Handbook, 8th Edition*. *PCI Design Handbook, 8th Edition*.

Kelleter, C., Burghardt, T., Binz, H., Blandini, L., & Sobek, W. (2020). Adaptive Concrete Beams Equipped With Integrated Fluidic Actuators. *Frontiers in Built Environment*, *6*(July), 1–13. https://doi.org/10.3389/fbuil.2020.00091

Steffen, S., Nitzlader, M., Burghardt, T., Binz, H., Blandini, L., & Sobek, W. (2021). An actuator concept for adaptive concrete columns. *Actuators*, *10*(10). https://doi.org/10.3390/act10100273